



ELSEVIER

Nuclear Instruments and Methods in Physics Research B 195 (2002) 389–399

---

**NIM B**  
Beam Interactions  
with Materials & Atoms

---

[www.elsevier.com/locate/nimb](http://www.elsevier.com/locate/nimb)

# Analysis of multiple scattering and multiphonon contributions in inelastic neutron scattering experiments

J. Dawidowski <sup>a,\*</sup>, G.J. Cuello <sup>b</sup>, M.M. Koza <sup>b</sup>, J.J. Blostein <sup>a</sup>, G. Aurelio <sup>a</sup>,  
A. Fernández Guillermet <sup>a</sup>, P.G. Donato <sup>c</sup>

<sup>a</sup> Consejo Nacional de Investigaciones Científicas y Técnicas, Centro Atómico Bariloche and Instituto Balseiro, Comisión Nacional de Energía Atómica, Universidad Nacional de Cuyo, 8400 S.C. de Bariloche, RN, Argentina

<sup>b</sup> Institut Laue Langevin, 6 rue Jules Horowitz, BP 156, 38042 Grenoble, France

<sup>c</sup> Universidad Nacional de la Patagonia “San Juan Bosco”, Comodoro Rivadavia – (9000), Argentina

Received 8 August 2001; received in revised form 15 March 2002

---

## Abstract

We present a method of analysis of inelastic neutron scattering (INS) experiments aiming at obtaining the density of phonon states in an absolute scale, as well as a reliable value of the mean-square displacement of the atoms. This method requires the measurement of the neutron total cross section of the sample as a function of energy, which provides a normalization condition for the INS experiment, as well as a value of the mean-square displacement. The method is applied in the case of an incoherent neutron scattering system, viz. the Ti–52wt.% Zr alloy. The applicability of this method to the study of metal alloys and other systems is discussed.

© 2002 Elsevier Science B.V. All rights reserved.

**PACS:** 78.70.N; 61.12.–q; 63.20; 29.30.h; 29.30.Hs; 61.25.Mv

**Keywords:** Debye–Waller factor; Inelastic neutron scattering; Neutron total cross section; Phonon density of states

---

## 1. Introduction

Inelastic neutron scattering (INS) techniques may be considered as the main route to access the vibrational properties of condensed matter. Inelastic scattering spectrometers, based either on pulsed or on stationary neutron sources, have nowadays achieved a high degree of development, thus allowing the attainment of high quality ex-

perimental data. Data obtained from such experimental devices provide, in principle, a direct information on the vibrational density of states, an essential magnitude in attempts to link microscopic to macroscopic phenomena. However, the nontrivial task to transform a magnitude expressed by a given number of neutron counts into a physically meaningful magnitude, is not yet fully developed. As a consequence, experimental results are seldom presented in an absolute scale. Attempts to use normalization standards such as vanadium samples [1] have proved to cause large errors (cf. [2]) due to the impossibility to reproduce

---

\* Corresponding author. Fax: +54-2944-445299.

E-mail address: [javier@cab.cnea.gov.ar](mailto:javier@cab.cnea.gov.ar) (J. Dawidowski).

the same geometry as the sample. Admittedly, multiple scattering and container effects play a major role in such discrepancies. It is a very well-known fact that multiple scattering and attenuation effects can be important even if all the reasonable cautions are taken in the sample design, since some low-signal portion of the observed spectra could nevertheless be seriously affected. An accurate calculation of them, can only be performed through numerical simulations containing a detailed description of the experimental setup [3,4]. For this reason, the employed procedure will strongly depend on the kind of spectrometer used to obtain the experimental data [5].

A different problem is posed when a vibrational density of states has to be extracted from the measured double-differential cross section. For this purpose it will always be necessary to perform multiphonon corrections, since it is mainly a temperature effect. Several algorithms based on iterative corrections were proposed in the past either for coherent [5–7] or incoherent [8] scatterers. The basic problem in such kind of corrections normally resides in the lack of a correct normalization criterion of the density of states, due to the fact that the measurement is either carried out in a limited range of energy transfers, which does not necessarily cover the whole vibrational spectrum, or in other cases the measurement is performed in a wide range but has a poor resolution for low-energy transfers. On the other hand, combination of results from different spectrometers, have also presented inconsistencies [9,10].

Neutron total cross section (NTCS) (i.e. the integral over all angles and energies of  $d^2\sigma/d\Omega dE$ ) is a magnitude that can be measured in a single transmission experiment over several decades in incident energy. A typical experiment can be rapidly performed in an intense neutron source, a fact that was recently employed to study real time phase changes [11]. Since the experimental results are free from multiple scattering and attenuation corrections, they provide a normalization condition for INS experiments in an absolute scale. Furthermore, it has recently shown its sensitivity to dynamic features of the density of states [12].

In this work we show the complete procedure of obtaining a well normalized density of states

starting from a measured inelastic cross section in a standard incoherent scatterer plus a total cross section of the same system. Multiple scattering and attenuation corrections are performed on the basis of previously published algorithms [5]. Special emphasis is made in the treatment of multiphonon corrections, which is the main topic of the present work. The procedure is based on a self consistent iterative algorithm on the INS data, but since it is unknown if all the dynamic features are comprised within the measured energy range, and as mentioned, INS experiments are subject to involved experimental corrections, the obtained values of the mean-square displacement of the atoms is compared with the experimental total cross section. The convergence of the process is thus double checked through the agreement with both INS and NTCS data. At the end of this process, an absolute normalization for the density of states is reached, together with a reliable value of the mean-square displacement. The relevance of NTCS data is stressed in connection with the different stages described in this procedure. Finally the extension of this method to coherent scatterers is discussed, and some applications of interest in materials sciences are suggested.

## 2. Experimental details

The sample under analysis was the binary alloy  $\text{Ti}_x\text{Zr}_{1-x}$  with  $x = 0.68$ , chosen to obtain a null mean scattering length, purely incoherently scattering sample. A Ti–52 wt.% Zr alloy was prepared from sponge Ti (99.9%) and Zr (99.9%) in an arc furnace, on a water-cooled copper hearth using nonconsumable electrodes under 350 Torr of Ar atmosphere. The alloy was then wrapped up in a Ta foil, encapsulated in quartz under high purity Ar and annealed for 3 h at 1273 K. In this way the structure of the alloy is expected to be that corresponding to thermodynamic equilibrium, viz. hexagonal closed packed (hcp) structure. A neutron activation analysis of impurities revealed the presence of less than 200 ppm of Hf, Cr, As and Mo, which contributes to the observed total cross section in less than 0.1%.

The inelastic scattering measurements were carried out at spectrometer IN6 (Institut Laue Langevin, Grenoble, France) at 300, 225 and 150 K with an incident neutron energy of 4.819 meV. The sample consisted on compacted shavings placed inside a cylindrical vanadium holder 10-mm diameter and 55-mm height. The observed range of energy transfers varied from 0 to 60 meV in neutron energy gain ('upscattering'). Empty can measurements were also performed and subtracted. Preliminary data processing of the experimental data, which consisted in monitor normalisation and change of time-of-flight scale into energy, was performed with standard software [13].

Due to the incoherence of the sample, the inelastic scattering profile had essentially the same shape in the energy scale, in the angular range from  $10^\circ$  to  $114^\circ$ , so the data for different angles were added into a single spectrum. In Fig. 1 we show the data obtained at different temperatures.

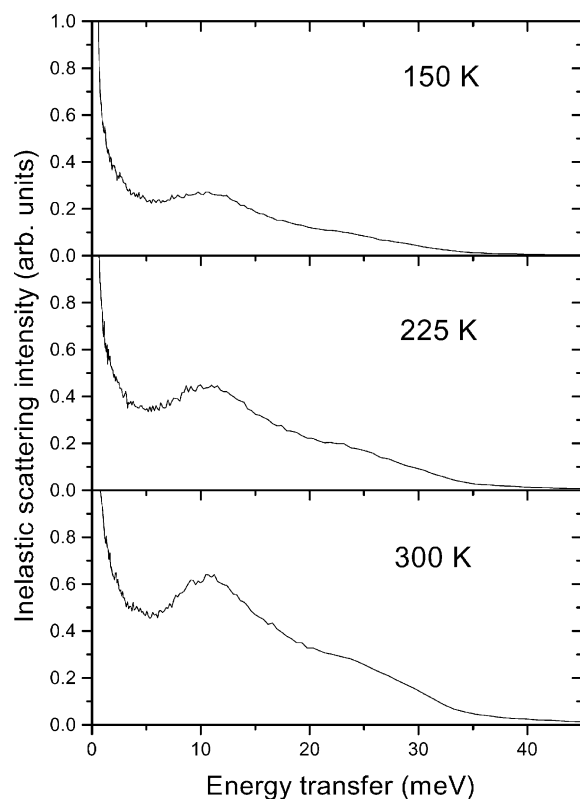


Fig. 1. Inelastic scattering spectra of Ti-52 wt.% Zr for 150, 225 and 300 K obtained at IN6.

The total cross section was measured in a transmission experiment at room temperature at the Bariloche electron LINAC facility (Argentina). The accelerator operated at a frequency of 25 Hz, and neutrons were thermalized in a 20 mm thick polyethylene moderator. The detector bank consisted of seven  $^3\text{He}$  proportional counters (10 atm filling pressure, 6" active length, 1" diameter). The sample was placed inside an aluminum can 4-cm diameter and 15-mm width. Measurements were carried out at room temperature, employing the 'sample in-sample out' technique [14] every 15 min. The background was measured inserting a beam shutter, and subtracted from the incident and the transmitted beam spectra. The neutron energy was determined by the time-of-flight technique, and spectra were stored in 8192 channels, 2- $\mu\text{s}$  width. The time of flight was corrected by mean

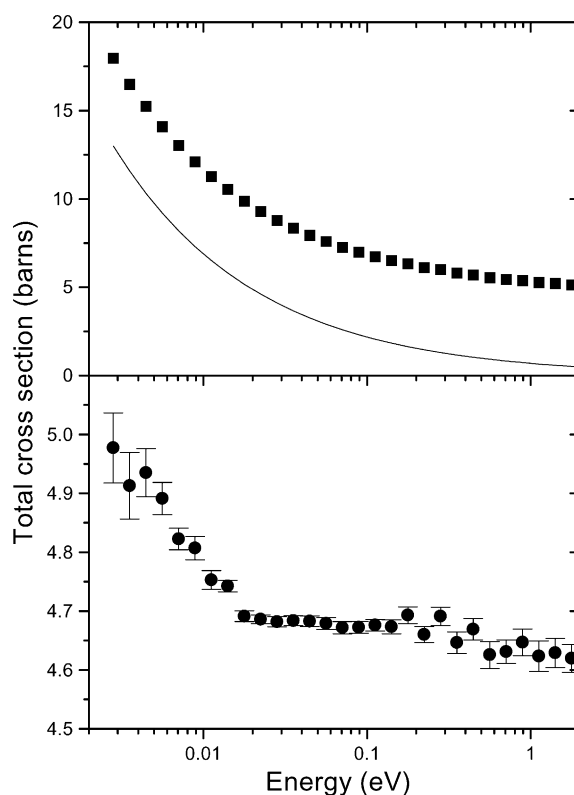


Fig. 2. Upper frame: measured total cross section (symbols) compared with the absorption component. Lower frame: scattering cross section.

emission time of the moderator, and the spectra were corrected by dead-time effects, which were less than 1% in every case.

The measured total cross section is shown in the upper frame of Fig. 2, where we also show the absorption component described by the expression [15]

$$\sigma_{\text{abs}}(E) = (x\sigma_{\text{abs}}^{\text{Ti}} + (1-x)\sigma_{\text{abs}}^{\text{Zr}}) \sqrt{\frac{0.0253\text{eV}}{E}}, \quad (1)$$

where  $E$  is the energy,  $\sigma_{\text{abs}}^{\text{Ti}} = 6.1$  barns and  $\sigma_{\text{abs}}^{\text{Zr}} = 0.185$  barns [16].

After subtracting the absorption component, we obtained the scattering total cross section that is shown in the lower frame of Fig. 2. For further discussions we here define the effective mass of our alloy, with the condition of satisfying the free gas behavior of the total cross section in the epithermal energy region [17]. This mass thus defined is 61.84 in neutron mass units.

### 3. Data processing

In this section, we will describe the steps followed to obtain the vibrational density of states starting from the INS and NTCS data.

#### 3.1. Multiple scattering and attenuation

Our approach makes use of a Monte Carlo code especially devised for the present configuration. The code was built on the principles described elsewhere [5] so we will only give a general outline here. The general magnitude measured in an ideal INS experiment is the double-differential cross section

$$\frac{d^2\sigma}{d\Omega dE} = \frac{N\sigma_b}{4\pi} \frac{k}{k_0} S(Q, \varepsilon), \quad (2)$$

where  $N$  is the total number of scattering centers,  $\sigma_b$  the bound-atom scattering cross section and  $k_0$  and  $k$  the modulus of the incident and emerging neutron wave vector respectively. As usual,  $Q$  is the impulse and  $\varepsilon$  the energy transferred by the neutron to the sample. The integral over all angles

and energies is the total cross section, which may be expressed as [12]

$$\sigma(E_0) = \frac{\sigma_b}{2k_0^2} \int_0^\infty Q dQ \int_{\varepsilon_{\min}}^{\varepsilon_{\max}} S(Q, \varepsilon) d\varepsilon, \quad (3)$$

where the energy limits of integration are the boundaries of the allowed kinematic range.

$$\begin{aligned} \varepsilon_{\max} &= \frac{\hbar^2 k_0 Q}{m} \left(1 - \frac{Q}{2k_0}\right), \\ \varepsilon_{\min} &= -\frac{\hbar^2 k_0 Q}{m} \left(1 + \frac{Q}{2k_0}\right). \end{aligned} \quad (4)$$

In principle, the scattering law  $S(Q, \varepsilon)$  would be directly accessible from INS experiments. Nevertheless, due to the finite size of the sample, the magnitude actually measured is the macroscopic double-differential cross section [3]

$$\frac{d^2\sigma}{d\Omega dE} = \frac{N\sigma_b}{4\pi A} \frac{k}{k_0} s(Q, \varepsilon), \quad (5)$$

which represents the probability that the neutron will leave the sample after any number of collisions, either in the sample or in the container material.  $A$  is the cross sectional area of the sample perpendicular to the incident beam, and the effective scattering law  $s(Q, \varepsilon)$  involves any number of collisions and it may be decomposed as follows:

$$s(Q, \varepsilon) = s_1(Q, \varepsilon) + s_M(Q, \varepsilon) + s_C(Q, \varepsilon), \quad (6)$$

where  $s_1(Q, \varepsilon)$  is the contribution of singly scattered neutrons,  $s_M(Q, \varepsilon)$  that of the multiple scattered and  $s_C(Q, \varepsilon)$  the contribution of the neutrons singly scattered in the can. As shown in [3] scattering as well as absorption processes are taken into account in Eq. (6).

The integral over all angles and energies of Eq. (5) is the fraction of neutrons interacting in the sample. By integrating both sides of Eq. (5) we obtain

$$1 - \mathcal{T}(E_0) = \frac{N\sigma_b}{2Ak_0^2} \int_0^\infty Q dQ \int_{\varepsilon_{\min}}^{\varepsilon_{\max}} s(Q, \varepsilon) d\varepsilon, \quad (7)$$

where  $\mathcal{T}(E_0)$  is the fraction of transmitted neutrons at energy  $E_0$ .

The goal in multiple-scattering corrections is to isolate the  $s_1(Q, \varepsilon)$  component, which is related to the desired scattering law through

$$s_1(Q, \varepsilon) = S(Q, \varepsilon)H(Q, \varepsilon), \quad (8)$$

where  $H(Q, \varepsilon)$  is the attenuation factor, which is the fraction of single-scattered neutrons that either fail to leave the sample due to multiple scattering and absorption, or are not detected due to the detector efficiency.

Following Copley's scheme [4], the Monte Carlo procedure devised to calculate multiple scattering and attenuation factors tracks individual neutron histories with a weight (initially 1), which decreases according to the attenuation suffered in the traversed path length. The path length is randomly obtained at each step using the exponential distributions derived from the macroscopic total cross sections of the material that the neutron has to traverse at the current energy. After each collision, the new energy and flight direction are decided from the distributions obtained from the energy-transfer kernels and double-differential cross sections for a mixture of ideal gases. For the purpose of the present alloy, this approach is accurate enough, although for other systems more elaborated models should be employed [18]. As shown in [5] the contribution of the current history to the detectors is evaluated at every step and the quantity to be scored is

$$z_i(Q, \varepsilon) = w_i P(E_i, E, \theta) \mathcal{T}(E, \mathbf{r}, \hat{\mathbf{k}}) C(E), \quad (9)$$

where  $w_i$  is the current history weight,  $\mathcal{T}(E, \mathbf{r}, \hat{\mathbf{k}})$  is the transmission factor for a neutron with energy  $E$ , placed at position  $\mathbf{r}$  inside the sample and traveling in the flight direction  $\hat{\mathbf{k}}$  and  $C(E)$  is the detector efficiency. The scattering probability  $P(E_i, E, \theta)$  must be described by a model as accurate as possible, since the sought results will depend on the shape of the proposed function. Furthermore, this probability function is the sought result itself, thus a suitable choice is a function based on the raw experimental data and the use of an iterative corrective method [19]. This choice is particularly convenient in the case of coherent scatterers, for which no simple theoretical model exists, with the condition that the spectrometer covers a sufficiently wide range in the  $Q - \omega$  plane, as discussed in [5]. In the present case, where we have a purely incoherent scatterer,

the probability function can accurately be described by a simple phonon expansion [12]

$$S(Q, \varepsilon) = e^{-\alpha Q^2} \delta(\varepsilon) + \sum_{n=1}^{\infty} \frac{1}{n!} e^{-\alpha Q^2} (\alpha Q^2)^n U_n(\varepsilon), \quad (10)$$

where  $\alpha$  is related to the Debye–Waller factor and the mean-square displacement through

$$\alpha = \frac{2W}{Q^2} = \frac{\langle u^2 \rangle}{3} = \frac{\hbar^2}{2M} \int_0^\infty \frac{Z(\varepsilon)}{\varepsilon} (2n(\varepsilon) + 1) d\varepsilon, \quad (11)$$

$n(\varepsilon)$  is the Bose occupation number,  $M$  is the mass of the scattering unit and the functions  $U_n(\varepsilon)$  are defined by

$$U_1(\varepsilon) = \begin{cases} \frac{\hbar^2}{2M\alpha} \frac{Z(\varepsilon)}{\varepsilon} (n(\varepsilon) + 1) & \text{for } \varepsilon \geq 0, \\ \frac{\hbar^2}{2M\alpha} \frac{Z(\varepsilon)}{\varepsilon} n(\varepsilon) & \text{for } \varepsilon < 0 \end{cases} \quad (12)$$

and

$$U_n(\varepsilon) = \int_{-\infty}^{\infty} U_{n-1}(\varepsilon') U_1(\varepsilon - \varepsilon') d\varepsilon', \quad (13)$$

where the functions  $U_n$  thus defined are properly normalized to unit area. From Eq. (10), it can be deduced that the value of  $\alpha$  will determine the number of terms for the phonon expansion necessary to converge. A preliminary estimate of  $\alpha$  was obtained by treating the alloy as a mixture of two elemental Debye solids, with the Debye energies taken from the literature [20]. In this way, a value of  $\alpha = 0.02 \text{ \AA}^2$  was obtained, which assured a good convergence with five terms in Eq. (10).

A first estimate for the  $Z(\varepsilon)$  function was obtained from the experimental data (which we will call  $S_{\text{exp}}(Q, \varepsilon)$ ), by considering only one term in the phonon expansion. Thus the expression

$$Z(\varepsilon) = \frac{C\varepsilon S_{\text{exp}}(Q, \varepsilon)}{Q^2 e^{-\alpha Q^2} (n(\varepsilon) + 1)} \quad (14)$$

was employed, where  $C$  is a normalization factor. Once the multiple scattering and empty can contributions, as well as the attenuation factor, were obtained, the experimental data were corrected

using Eqs. (6) and (8). Starting from this first step, an iterative method is proposed, in which the function  $Z(\varepsilon)$  is determined from the data corrected for multiple scattering and attenuation, and for multiphonon effects, which will be described in the next subsection. To finish the description of the multiple scattering corrections, it is useful to summarize the input data involved in the calculation:

- geometric description of the sample and detector bank,
- detector efficiency as a function of neutron energy,
- scattering and absorption total cross-sections for sample and sample-holder materials as a function of neutron energy,
- energy limits for the significant values of the energy-transfer kernels, for sample and sample-holder materials as functions of neutron energy,
- phononic functions  $U_n(\varepsilon)$  as functions of energy. (In our case, the first five terms of the expansion.)

### 3.2. Multiphonon corrections

The starting function we will use for multiphonon corrections is calculated from the experimental data corrected by multiple scattering and attenuation effects  $S'_{\text{exp}}(Q, \varepsilon)$ . It is defined as

$$U_1^{(0)}(\varepsilon) = \frac{CS'_{\text{exp}}(Q, \varepsilon)}{Q^2 e^{-\alpha Q^2}}, \quad (15)$$

where  $C$  is a normalization constant.  $U_1^{(0)}(\varepsilon)$  would be exactly equal to  $U_1(\varepsilon)$  if no multiphonon effects were present. Since the experimental data are in the upscattering region, we have to complete the corresponding down-scattering branch by the detailed balance condition.

Multiphonon terms are calculated by convolution (Eq. (13)), and the total multiphonon contribution is

$$U_m^{(0)}(\varepsilon) \approx \sum_{n=1}^5 U_n^{(0)}(\varepsilon). \quad (16)$$

The input data are corrected by a factor [7]

$$U_1^{(1)}(\varepsilon) = \frac{U_1^{(0)}(\varepsilon)}{1 + \frac{U_m^{(0)}(\varepsilon)}{U_1^{(0)}(\varepsilon)}}. \quad (17)$$

The new value of the one-phonon function thus defined serves as input of an iterative process, where the output of the calculation step  $n$  is related with the one at step  $n - 1$  through

$$U_1^{(n)}(\varepsilon) = \frac{U_1^{(0)}(\varepsilon)}{1 + \frac{U_m^{(n-1)}(\varepsilon)}{U_1^{(n-1)}(\varepsilon)}}. \quad (18)$$

The process typically converges after a few iterations.

### 3.3. Normalization condition from total cross section experiments

As shown in the preceding paragraphs the magnitude of multiphonon corrections will critically depend of the value of  $\alpha$ . As a result of the above mentioned procedure, a value of  $\alpha$  will, in principle, be obtained, if it is accepted that the range of measured energy transfers covers the whole vibrational energy range, which will not always be the case. Moreover, inspection of Eq. (11) reveals that in order to calculate  $\alpha$  we require a good knowledge of the density of states, especially in the low energy region, where the elastic peak normally hides such information. Bearing in mind these facts, and also that INS data have to be corrected by the nontrivial multiple scattering and attenuation corrections, it will always be desirable, or absolutely necessary to have a value of  $\alpha$  obtained from an alternative experimental source, either to check the consistency of the results obtained from the multiphonon corrections or to give information of this essential value.

In Section 3.1, we showed that NTCS data as a function of energy are necessary to perform multiple scattering and attenuation corrections. On the other hand, NTCS is closely related with the value of  $\alpha$ . This can be verified by calculating the integral defined in Eqs. (3) and (4), with the expansion (10)

$$\sigma(E_0) = \frac{\sigma_b}{2k_0^2} \sum_{n=1}^{\infty} \frac{1}{n!} \alpha^n \int_0^{\infty} dQ Q^{2n+1} e^{-\alpha Q^2} \times \int_{\varepsilon_{\min}}^{\varepsilon_{\max}} U_n(\varepsilon) d\varepsilon. \quad (19)$$

This expression was already employed in [12] to show the potentiality of the NTCS technique to provide information on the dynamics of the systems under study. In the present case Eq. (19) gives us a means to check  $\alpha$ .

## 4. Results

In this section, we describe the results obtained in the different calculation steps. We will restrict ourselves to the details of the 300 K measurement.

### 4.1. Multiple scattering and attenuation effects

In the first step we obtained an estimation of the density of states  $Z(\varepsilon)$  from the experimental data according to Eq. (14), which is shown in Fig. 3. In the lower frame of Fig. 3 we show the five terms used in the phonon expansion (Eq. (10)), excluding the elastic term) to describe the function  $S(Q, \varepsilon)$  in the Monte Carlo code. In this first step the preliminary value  $\alpha = 0.02 \text{ \AA}^2$  was used, as explained in Section 3.1, which was refined in further steps.

Monte Carlo results are shown in Fig. 4, for the mean scattering angle of  $62.5^\circ$  where we show single, multiple and total scattering curves, as well as the attenuation coefficient in the inset. Runs were performed at several angles showing similar results. The main features of the obtained results are:

- The total scattering curve has essentially the same shape as its multiple scattering component with a factor 8.6 between them with an error less than 1% in all the explored energy range.
- The attenuation coefficient varies a 5% in all the explored energy range, and less than 2% in the range from 0 to 40 meV, where the density of states exhibits its main features.

Therefore we conclude that multiple scattering effects do not significantly affect the shape of the observed inelastic spectrum.

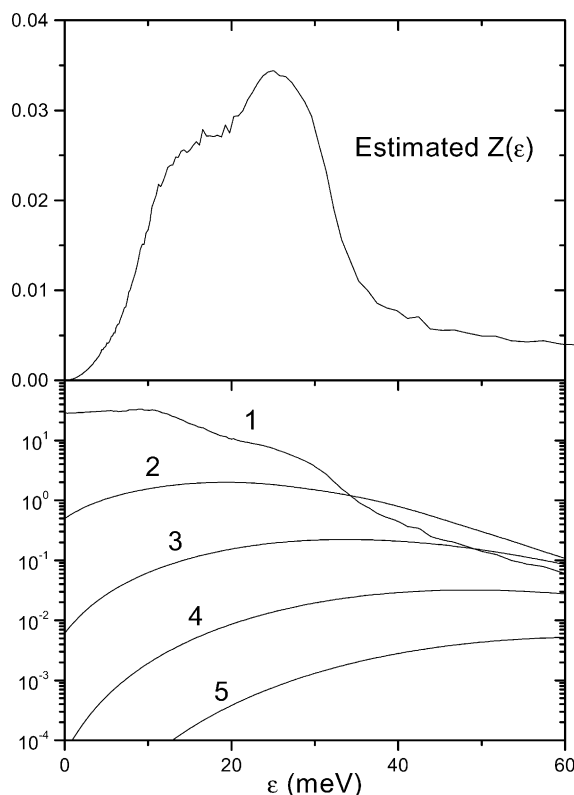


Fig. 3. Upper frame: first estimation of the density of states, from the experimental data and the preliminary value of  $\alpha = 0.02 \text{ \AA}^2$ . Lower frame: first five terms of the phonon expansion.

### 4.2. Multiphonon effects

Starting from Eq. (15) we followed the iterative process described in Section 3.2. As already mentioned, the starting value of  $\alpha$  was  $0.02 \text{ \AA}^2$ , and the mass was that indicated in Section 2. This process continues until no significant changes between iterations are observed. In Fig. 5 we show the final result for  $U_1$ ,  $U_m$  and  $U_{\text{total}}$  multiplied by the factor  $\varepsilon/n(\varepsilon)$  in order to directly compare the results with a density of states. The value of  $\alpha$  for which the convergence was attained is  $0.0095 \text{ \AA}^2$ . The starting function  $U'_1$  is not shown in the graph because it agrees within the line thickness with  $U_{\text{total}}$ . For comparison, in the inset of the same figure we show the results from the initial guess of  $\alpha$  ( $0.02 \text{ \AA}^2$ ). A large overestimation of multiphonon effects is observed.

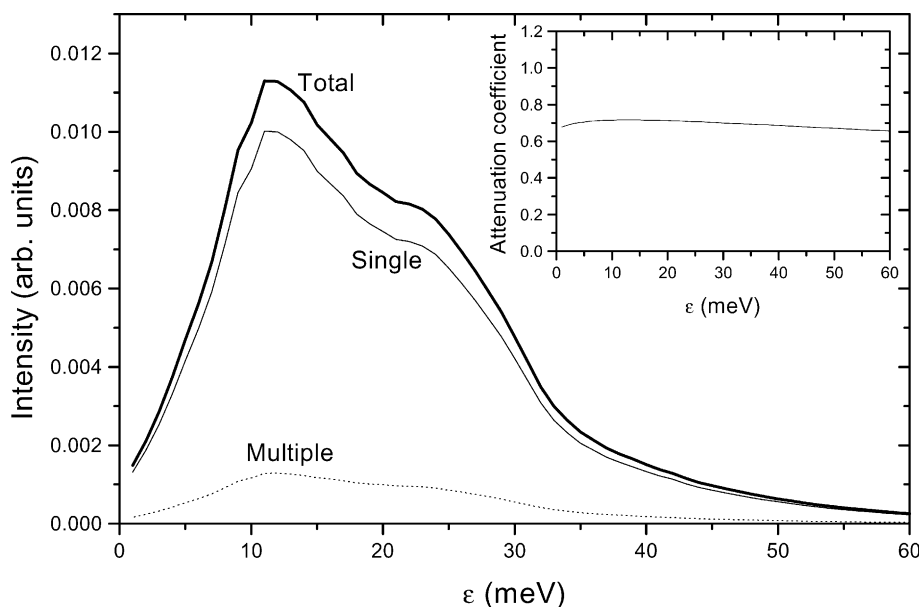


Fig. 4. Monte Carlo results showing single- and multiple-scattering components, and the total scattering curve. Inset: the attenuation coefficient.

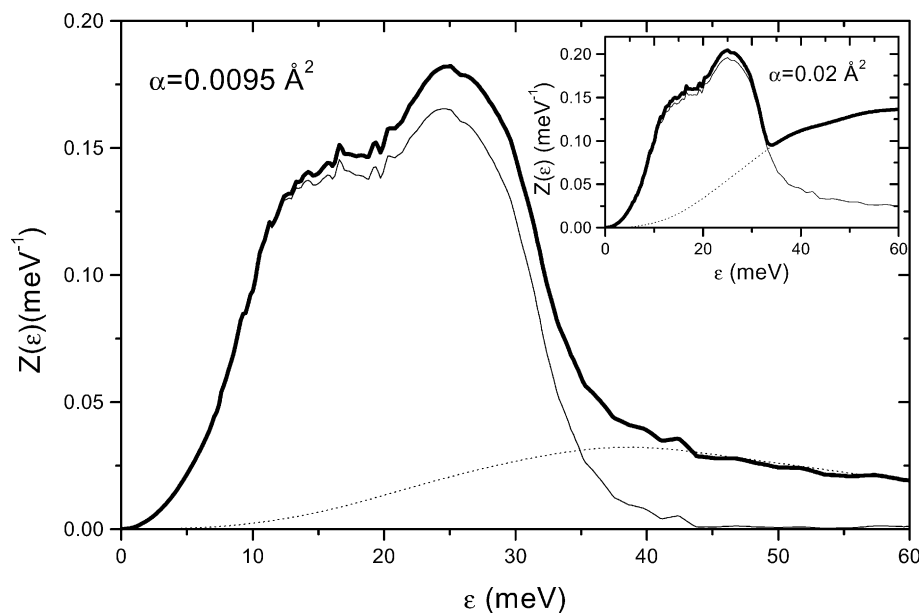


Fig. 5. Results of multiphonon calculations for  $\alpha = 0.0095 \text{ \AA}^2$ ; thin line: one-phonon, dotted line: multiphonon, thick line: total. In the inset, the results of the first estimate ( $\alpha = 0.02 \text{ \AA}^2$ ) showing the excess in the multiphonon component.

A comment on the error of the value of  $\alpha$  obtained in this process seems in order. As it was previously stated, the elastic peak conceals the

low-frequencies data, so an extrapolation to low energies in the experimental function (Eq. (15)) must be performed. In the limit where no mul-

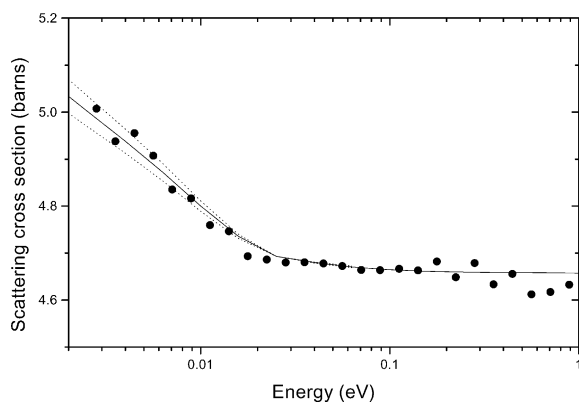


Fig. 6. Measured scattering total cross section compared with calculations based on the density of states obtained in the inelastic measurement. Solid curve shows the results for  $\alpha = 0.0095 \text{ \AA}^2$ , and the upper and lower dotted curves for  $0.00105$  and  $0.0085 \text{ \AA}^2$ , respectively.

tiphonon effects exist, this function must reach some constant value given by the Debye model. We tried out several extrapolations around the base of the elastic peak at about 3 meV and we observed a variation in the resulting  $\alpha$  of about  $0.0005 \text{ \AA}^2$ .

Finally, as we stated in the previous section, we checked the density of states resulting from the inelastic measurement by calculating the total cross section and comparing it with our experimental results (Fig. 6). In addition to the good agreement observed by setting  $\alpha = 0.0095 \text{ \AA}^2$  in the calculation, we trace the sensibility of the NTCS method by comparing with calculations performed using  $\alpha = 0.0085 \text{ \AA}^2$  and  $\alpha = 0.0105 \text{ \AA}^2$ . These results are in good agreement with the ones obtained in INS experiments, what means that in our INS experiment all significant features of the vibrational spectrum were included in the measured energy-transfer range.

## 5. Discussion

In this paper, we described a procedure devised to obtain the vibrational density of states combining the data obtained from an INS and a NTCS experiment, in an absolute scale. In the process, a value of the mean-square displacement was refined

starting from a rough estimate. In the present case we analyzed the treatment of an incoherent scatterer, which allows the description through a simple phonon expansion in the incoherent approximation, in the models employed for multiple scattering and multiphonon corrections. In all the described calculation steps, NTCS data play a multiple role related with the required absolute normalization viz.

- it provides the normalization condition for experiments that involve final angle and energy analysis;
- it gives the information of the neutron mean-free-path as a function of the energy, to be applied in Monte Carlo multiple-scattering simulations;
- it serves to obtain the mean-square displacement.

One of the essential results of the present paper is that the initial estimate of the  $\alpha$  quantity, viz.  $\alpha = 0.02 \text{ \AA}^2$ , was significantly modified by the procedure described above. The final value for this Ti–Zr alloy, viz.  $\alpha = 0.0095 \text{ \AA}^2$  is comparable with known values for the elements Ti and Zr, viz.  $0.0066$  and  $0.0073 \text{ \AA}^2$  [22–24], respectively. We conclude that the present procedure yielded a plausible value for the Ti–Zr alloy. As it was already mentioned, the fact that the value of  $\alpha$  obtained from the multiphonon refinement is in agreement with the one obtained from NTCS data, means that the energy-transfer range of INS data comprises the whole  $Z(\varepsilon)$ . If some portion of  $Z(\varepsilon)$  were out of the measured range, we could not have performed a correct normalization of the density of states. In such cases the value of  $\alpha$  obtained from the NTCS data, has to be introduced in Eq. (11) to get the correct normalization of the measured portion of the density of states. This, in turn, affects the normalization of the phonon functions (12) and (13). Multiphonon corrections are still possible to be performed within the measured dynamic range, although no value of  $\alpha$  is refined in the process.

We hope that the procedure prescribed in this paper will be a useful tool to improve the accuracy in the analysis of INS data, and will allow to give a

further step in the usual analysis procedures by providing the means to express the results in an absolute scale, even in those cases where the measurements are performed in an energy-transfer range that does not comprise all the relevant dynamic range, or in situations where the  $\alpha$  parameter is difficult to be known such as in the case of systems with meta-stable structures.

It is worth to mention that an extension of the present method for coherent scattering can be accomplished in line with previous works (see Refs. [5,21]). In those papers resource was made of values of the mean-square displacements obtained from different techniques, but a better refinement would have been achieved if advantage was taken of NTCS data. In such cases due to the complexity of the scattering laws, a description starting from the raw experimental data plus an iterative refinement are required, instead of the simple model here employed.

## 6. Final remarks on applications and future work

In the previous section, we referred to the possibility of a systematic investigation of the  $\alpha$  parameter for transition metal alloys. Here the case will be highlighted of the alloys formed by an element of the Ti-group (i.e. Ti, Zr or Hf) with other metals placed to the right in the periodic table. At high temperatures these alloys present a stable body centered cubic (bcc) phase, which on rapid cooling to room temperature undergoes diffusionless transitions originating two new structures. One of the structures is the hcp phase studied in the present work. The second structure is often called omega ( $\Omega$ ) phase and it has been the subject of considerable experimental and theoretical interest [25]. Much of the recent work on the  $\Omega$  structure, which is a meta-stable phase in these alloy systems, focussed on the structural and other equilibrium properties [26–33]. Contrasting with this, very little is known on the vibrational properties of  $\Omega$  and those of the parent bcc phase. In this context, the method proposed in the present paper may be considered as a useful alternative. More specifically, the present procedure should be particularly appropriate to get  $\alpha$  values as a func-

tion of the composition in alloys of the prototype systems Zr–Nb and Ti–V. Both systems have been extensively studied with neutron diffraction techniques, and detailed characterizations have been presented of the structural properties and the phase occurrence systematics in quenched alloys [26–28,30]. By changing the alloy content it should be possible to determine  $\alpha$  values for one-phase alloys (i.e. bcc at the Nb or V rich end) or two-phase alloys (i.e. bcc +  $\Omega$  for Nb or V contents of the order of 10 at.%). Some  $\alpha$  values for the bcc phase in these systems have been reported [34] which could be used to compare with the new results, thus adding to the credibility of the  $\alpha$  values for the  $\Omega$  phase, which are not known from direct measurements. Further applications from the present technique stem from the possibility of studying the mean-square displacement of atoms in those materials, where either due to the lack of crystallinity or in the case of incoherent scatterers, methods based on diffraction techniques fail to provide results. In this context, it is worth to mention the study of amorphous or hydrogenous materials.

## Acknowledgements

We are especially grateful C.O. Ayala who prepared the samples employed in the experiments. L. Capararo is acknowledged for the technical support and M. Schneebeli and P.D'Avanzo for the LINAC operation. We thank M. Arribère for performing the neutron activation analysis. We wish to acknowledge support from ILL and the access to the beamtime. We also thank S. Jenkins for his technical support during the IN6 experiment. This work was supported by ANPCyT (Argentina) under Project PICT no. 03-4122, and CONICET (PEI 149/98).

## References

- [1] P. Verkerk, A.A. Van Well, Nucl. Instr. and Meth. B 228 (1985) 438.
- [2] C. Benmore, B. Mos, P. Egelstaff, P. Verkerk, J. Neutron Res. 6 (1998) 279.
- [3] V.F. Sears, Adv. Phys. 24 (1975) 1.

- [4] J.R.D. Copley, Comput. Phys. Commun. 7 (1974) 289; J.R.D. Copley, P. Verkerk, A.A. Van Well, H. Fredrikze, Comput. Phys. Commun. 40 (1986) 337.
- [5] J. Dawidowski, F.J. Bermejo, J.R. Granada, Phys. Rev. B 58 (1998) 706.
- [6] D.L. Price, J.M. Carpenter, J. Non Cryst. Sol. 92 (1987) 153.
- [7] J. Dawidowski, F.J. Bermejo, R. Fayos, R. Fernández Perea, S.M. Bennington, A. Criado, Phys. Rev. E 53 (1996) 5079.
- [8] J. Wuttke, M. Kiebel, E. Bartsch, F. Fujara, W. Petry, H. Sillescu, Z. Phys. B 91 (1993) 357.
- [9] F.J. Bermejo, J.C. Dore, W.S. Howells, P. Chieux, E. Enciso, Physica B 156&157 (1987) 154.
- [10] R.L. McGreevy, The tertiary spectrometer: the role of the software in the design and performance of instruments and experiments, International Conference on Neutron Scattering, Munchen, Germany, 2001.
- [11] K. Meggers, H.G. Priesmayer, M. Stalder, S. Vogel, W. Trela, Physica B 234–236 (1997) 1160.
- [12] J. Dawidowski, J.R. Santisteban, J.R. Granada, Physica B 271 (1999) 212.
- [13] D. Richard, G. J. Kearley, M. Ferrand, LAMP Large Array Manipulation Program, Institut Laue Langevin, 1995.
- [14] F. Kropff, J.R. Granada, L.A. Remez, A. Vasile, Annals of Nuclear Energy 3 (1976) 55.
- [15] S.F. Mughabghab, N. Divadeenam, N.E. Holden, Neutron Cross Sections, Academic Press, New York, 1981.
- [16] K. Knopf, W. Waschowski, J. Neutron Res. 5 (1997) 147.
- [17] J.R. Granada, Z. Naturforsch. 39a (1984) 1160.
- [18] J.R. Granada, Phys. Rev. B 31 (1985) 4167.
- [19] M. Russina, F. Mezei, Neutrons and numerical methods, M.R. Johnson, G.J. Kearley, H.G. Büttner (Eds.), AIP Conference Proceedings, Vol. 479, p. 47, (1999).
- [20] N.W. Ashcroft, N.D. Mermin, Solid State Physics, Harcourt Brace College Publishers, Orlando, 1976.
- [21] J. Dawidowski, F.J. Bermejo, C. Cabrillo, S.M. Bennington, Chemical Physics 258 (2000) 247.
- [22] V.F. Sears, S.A. Shelley, Acta Cryst. A 47 (1991) 441.
- [23] L.-M. Peng, G. Ren, S.L. Dudarev, M.J. Whelan, Acta Cryst. A 52 (1996) 456.
- [24] A. Fernández Guillermet, G. Grimvall, Phys. Rev. B 40 (1989) 1521.
- [25] S.K. Sikka, Y.K. Vohra, R. Chidambaram, Prog. Mat. Sci. 27 (1982) 245.
- [26] G.M. Benites, A. Fernández Guillermet, G.J. Cuello, J. Campo, J. Alloys Comp. 245 (2000) 183.
- [27] G.M. Benites, A. Fernández Guillermet, J. Alloys Comp. 302 (2000) 192.
- [28] G. Aurelio, A. Fernández Guillermet, Scripta Mat. 43 (7) (2000) 665.
- [29] G. Aurelio, A. Fernández Guillermet, Z. Metallkd. 91 (2000) 35.
- [30] G. Aurelio, A. Fernández Guillermet, G.J. Cuello, J. Campo, Met. Trans. A 33 (5) (2002) 1307.
- [31] J.E. Garcés, G.B. Grad, A. Fernández Guillermet, S.J. Sferco, J. Alloys Comp. 287 (1999) 6.
- [32] J.E. Garcés, G.B. Grad, A. Fernández Guillermet, S.J. Sferco, J. Alloys Comp. 289 (1999) 1.
- [33] G.B. Grad, P. Blaha, J. Luitz, K. Schwarz, A. Fernández Guillermet, S.J. Sferco, Phys. Rev. B 62 (2000) 12743.
- [34] J. Trampenau, Ph.D. Dissertation, Universität Münster, 1991.